The Astrophysical Journal, 661: L101–L104, 2007 May 20

DEPLETED CARBON MONOXIDE IN FRAGMENT C OF THE JUPITER-FAMILY COMET 73P/SCHWASSMANN-WACHMANN 3

M. A. DiSanti,[1] W. M. Anderson,[1,2] G. L. Villanueva,[1] B. P. Bonev,[1,2]
K. Magee-Sauer,[3] E. L. Gibb,[4] and M. J. Mumma[1]

Received 2007 February 9; accepted 2007 April 6; published 2007 May 4

ABSTRACT

Carbon monoxide emission was targeted in fragment C of the recently split Jupiter-family comet 73P/Schwassmann-Wachmann 3 during its 2006 apparition, using the Cryogenic Echelle Spectrograph (CSHELL) at the NASA IRTF on Mauna Kea, Hawaii. Simultaneous sounding with H_2O near 4.65 μm revealed highly depleted CO, consistent with a mixing ratio of 0.5% $\pm$ 0.13%. Along with depleted CH_3OH but nearly normal HCN, this may indicate that this comet formed in the inner giant planets' region or, alternatively, that it formed relatively late, after significant clearing of the protosolar nebula.

Subject headings: comets: general — comets: individual (73P/Schwassmann-Wachmann 3) — molecular processes — solar system: formation

Online material: color figure

1. INTRODUCTION

The ubiquitous nature and high volatility of carbon monoxide make it a principal probe of thermal conditions in cold dense cloud cores, from which planetary systems arise (e.g., Gibb et al. 2004 and references therein), and in circumstellar disk environments (Shuping et al. 2001; Salyk et al. 2006). Comets presumably formed under similar conditions in our own nascent solar system; however, tracing cometary origins is complicated by their radial migration in the protoplanetary disk and by dynamical interactions with the growing giant planets (see Gomes et al. 2005). Such interactions placed comets into two principal present-day reservoirs: the Oort Cloud and the Edgeworth-Kuiper Belt, where they remain largely unaltered until perturbed into the inner solar system (see Gladman 2005).

Spectroscopic studies reveal chemical diversity among comets (e.g., Biver et al. 2002; Mumma et al. 2003), so building a taxonomy based on cometary composition can provide fundamental clues to natal conditions and constrain dynamical models of solar system formation and evolution. CO is the most volatile parent species routinely measured in comets, making it a particularly sensitive indicator of the thermal conditions experienced by the precometary ices and perhaps of postaccretional processing.

Kuiper Belt objects (KBOs) are sampled through observations of comets belonging to Jupiter's dynamical family, a transitional population fed primarily from the scattered Kuiper disk (Bernstein et al. 2004). These comets tend to have lower production rates than Oort Cloud comets due to their smaller sizes, perhaps coupled with increased processing of their surface layers resulting from frequent and numerous perihelion passages. This makes Jupiter family comets (JFCs) more observationally challenging.

In spring 2006, the JFC 73P/Schwassmann-Wachmann 3 (hereafter SW3) passed within 0.1 AU of Earth, providing an excellent opportunity to measure its volatile composition in detail. SW3 generated particular interest because of its history of (ongoing) fragmentation events, first seen during its 1995 apparition (Boehnhardt & Kaufl 1995; Crovisier et al. 1996; Boehnhardt et al. 2002). This ongoing fragmentation exposed relatively fresh (and perhaps more pristine) cometary material, and therefore our measurements could have cosmogonic implications.

In 2006, fragment B exhibited several outbursts and rapid disintegration (Weaver et al. 2006), while fragment C showed more stable behavior, stimulating searches for causal factors such as possible chemical heterogeneity. Observations of fragments B and C were conducted, emphasizing parent volatiles with emissions in the range 2.9–3.7 μm (e.g., H_2O, C_2H_6, C_2H_2, HCN, CH_3OH, H_2CO, CH_4); however, no significant compositional differences were seen (Blake et al. 2006; Villanueva et al. 2006a; Kawakita et al. 2006a, 2006b; Dello Russo et al. 2006). In this Letter, we report a sensitive search for CO emission in fragment SW3-C based on simultaneous observation of emission in the $v = 1$–0 band and water hot-band emission near 4.646 μm.

2. OBSERVATIONS AND ANALYSIS

Fragment SW3-C[5] was observed with the long-slit Cryogenic Echelle Spectrograph (CSHELL; Tokunaga et al. 1990) at the NASA Infrared Telescope Facility (IRTF) on 2006 May 27 and 30. The late-May period was chosen because of the comet's proximity to perihelion, its small geocentric distance (Δ), and (especially) its nonzero geocentric velocity ($\dot{\Delta}$) that is essential for displacing cometary CO lines from their (opaque) telluric counterparts.[6] We tuned CSHELL to simultaneously encompass emissions from both CO and H_2O (Fig. 1), ensuring that the retrieved mixing ratio for CO was independent of systematic effects such as uncertainties in absolute flux calibration and slit losses. We used our standard algorithms to process the spectra (e.g., DiSanti et al. 2001; see also Villanueva et al. 2006a).

[1] Solar System Exploration Division, NASA Goddard Space Flight Center, Code 693, Greenbelt, MD 20771; disanti@ssedmail.gsfc.nasa.gov.
[2] Department of Physics, Catholic University of America, Washington, DC 20064.
[3] Department of Physics and Astronomy, Rowan University, Glassboro, NJ 08028.
[4] Department of Physics and Astronomy, University of Missouri at St. Louis, St. Louis, MO 63121.

[5] CO observations of fragment B were also attempted; however, it was several magnitudes fainter than fragment C, so a meaningful constraint was not achievable in the time available.
[6] Insufficient geocentric Doppler shift precluded measuring CO near closest approach to Earth (earlier in May), when SW3 was brightest.

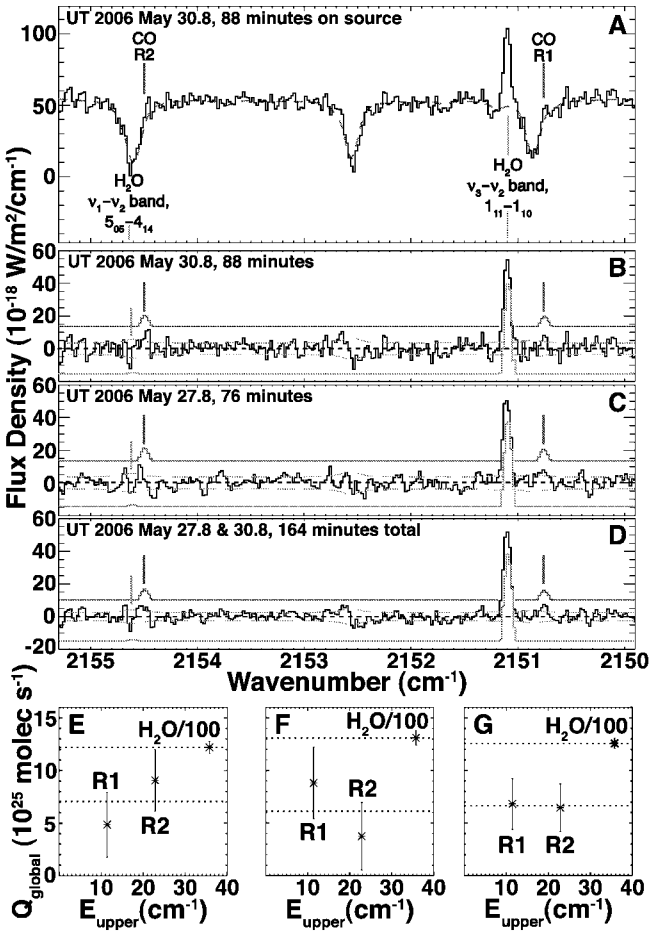

FIG. 1.—(*a*) Spectral extract (*solid trace*) of signal contained in a 1″ × 3″ aperture centered on the nucleus, with Doppler-shifted positions of CO and H_2O lines indicated. Subtracting the modeled transmittance (*dashed trace*) convolved to the spectral resolving power of the observations ($\lambda/\Delta\lambda = 2.8 \times 10^4$ on May 27 and 2.6×10^4 on May 30) yields the net molecular emission (*b–d*, *solid traces*). Also shown in panels *b–d* are the modeled CO (above the comet residuals) and H_2O (below the residuals) for $T_{rot} = 80$ K, and the 1 σ stochastic noise envelope (*dashed traces*). (*e–g*): Excitation plots corresponding to panels *b–d*, respectively, showing line-by-line global production rates at 80 K (with ± 1 σ stochastic errors) for CO (labeled "*R*1" and "*R*2") and for H_2O (divided by 100) vs. upper state rotational energy. For all points, the residual signal is integrated over seven spectral channels (~0.15 cm^{-1}) centered on the Doppler-shifted line frequency. The horizontal dotted lines indicate the global *Q* for H_2O (*upper line*) and the weighted mean Q_{global} for CO (*lower line*). [*See the electronic edition of the Journal for a color version of this figure.*]

Subtracting a synthetic transmittance function[7] from the observed comet spectrum (Fig. 1*a*) isolated molecular emission in excess of the continuum (Figs. 1*b*–1*d*).

We measured a weak yet positive signal at each Doppler-shifted CO line frequency (Figs. 1*e*–1*g*). Determining the production rate (*Q*) of a parent volatile requires comparison of measured spectral line intensities with those predicted by a quantum mechanical molecular fluorescence model at various rotational temperatures (T_{rot}) (see Dello Russo et al. 2004 and DiSanti et al. 2006 for detailed discussions). The CO lines targeted in SW3 sample closely spaced rotational energies (~11 and 23 cm^{-1} for the upper states of *R*1 and *R*2, respectively), so we were not able to obtain a meaningful measure of T_{rot}. Instead, we present results for a range of plausible temperatures (Table 1) based on T_{rot}-values reported for SW3-C near a heliocentric distance $R_h = 1$ AU (Kawakita et al. 2006a, 2006b; Dello Russo et al. 2006).

Our production rate for H_2O relied on the strong line with rest frequency 2151.194 cm^{-1} (Fig. 1) and rotational energy $E_{upper} \sim 36$ cm^{-1}. A "nucleus-centered" *Q* was calculated assuming spherically symmetric gas in the coma expanding with speed $v_{gas} = 650$ m s^{-1} (based on velocity-resolved line profiles; see Biver et al. 2006; G. L. Villanueva et al. 2007, in preparation). To account for slit losses, a growth factor (q_{scale}, determined from the spatial distribution of H_2O emission about the nucleus) was applied to yield the total (global) *Q* for H_2O (Dello Russo et al. 2004; Bonev et al. 2006, Appendix B). Since CO and H_2O were measured (simultaneously) in the same instrument setting, we used this growth factor to correct for slit losses in the CO nucleus-centered flux and to obtain the global *Q* for CO. Our results therefore pertain to the abundance of CO housed as ice in the nucleus (i.e., the native CO abundance).

Our analysis of CO accounted for possible contamination from a second H_2O line (rest frequency 2154.711 cm^{-1}; $E_{upper} \sim 320$ cm^{-1}) partially blended with the *R*2 line of CO. We subtracted its modeled intensity (convolved to the instrumental resolving power) from the observed comet residuals to obtain the net *R*2 line intensity (see Table 1, note e).

3. DISCUSSION

Our results indicate a depleted abundance of carbon monoxide in comet SW3-C ($CO/H_2O \cong 0.5\%$, at the ~4 σ confidence level; Table 1). This represents the most stringently constrained mixing ratio yet reported for CO based on NIR comet observations, although comparably low values were reported from UV observations of the Oort Cloud comets D/1999 S4 (LINEAR) (Weaver et al. 2001), C/2000 WM_1 (LINEAR), and C/2001 A2 (LINEAR) (Weaver et al. 2002).[8]

Our observations complement other studies of parent volatiles in comet SW3. In the NIR, these emphasized the multitude of organic molecules (i.e., HCN, NH_3, C_2H_2, CH_4, C_2H_6, H_2CO, and CH_3OH, in addition to H_2O and prompt OH) having rovibrational emissions in the region 2.8–3.7 μm (Villanueva et al. 2006a; Kawakita et al. 2006a, 2006b; Mumma et al. 2006; Dello Russo et al. 2006). Submillimeter and radio observations also quantified several of these species along with other molecules (Villanueva et al. 2006b; Biver et al. 2006; Crovisier et al. 2006). Together, these studies revealed that SW3 was depleted in organic volatiles, excepting HCN.

3.1. *Relation to Oxidized Carbon Chemistry*

Measuring H_2CO and CH_3OH in addition to CO can provide us with information on the formation environment of comets, particularly when examined in the context of their overall volatile composition. Prior to being incorporated into the nucleus, CO may be converted to these chemically linked molecules through H-atom surface addition reactions on icy precometary grains, a process analogous to that proposed for the formation of C_2H_6 from C_2H_2 (Mumma et al. 1996). Laboratory experiments show hydrogenation of CO to be efficient only at very low temperatures (~10–20 K), the yields being highly dependent on the density (i.e., fluence) of atomic hydrogen, on tem-

[7] The spectral transmittance was synthesized using the GENLN2 ver. 4 line-by-line code (Edwards 1992), which accesses the HITRAN-2004 Molecular Database (Rothman et al. 2005). Telluric water burdens of 1.5 and 2.3 precipitable millimeters were used on May 27 and 30, respectively.

[8] For C/2001 A2 (LINEAR), the UV CO abundance differed substantially from IR results ($CO/H_2O \sim 3\%$–4%), for which CO and H_2O were measured simultaneously (Magee-Sauer et al. 2007).

TABLE 1
PRODUCTION RATES FOR H_2O AND CO IN FRAGMENT C OF COMET 73P/SCHWASSMANN-WACHMANN 3

UT Date[a] 2006	t_{int} (minutes)	T_{rot} (K)	Molec. Line	F_{line}[b] (10^{-19} W m^{-2})	Q[c] (10^{25} molecules s^{-1})	Relative Abundance[d]
May 27.8	76	80	H_2O	47.0 ± 2.5	1310 ± 69 (229)	100
(R_h = 0.952)			CO *R*1	8.4 ± 3.3	8.8 ± 3.4 (3.7)	
($\dot{\Delta}$ = 0.148)			*R*2[e]	4.4 ± 3.8	3.7 ± 3.2 (3.3)	
(Δ = +12.5)			*R*1+*R*2[e]	12.9 ± 5.0	6.1 ± 2.3 (2.7)	0.47 ± 0.19
May 30.8	88	80	H_2O	48.9 ± 2.4	1220 ± 59 (224)	100
(R_h = 0.946)			CO *R*1	5.2 ± 3.3	4.9 ± 3.1 (3.2)	
($\dot{\Delta}$ = 0.171)			*R*2[e]	12.0 ± 3.9	9.1 ± 2.9 (3.3)	
(Δ = +13.1)			*R*1+*R*2[e]	17.2 ± 5.0	7.1 ± 2.1 (2.5)	0.58 ± 0.18
May 27 and 30[f]	164	60	H_2O	48.0 ± 1.7	1150 ± 41 (146)	
			CO[e]	15.0 ± 3.5	5.6 ± 1.3 (1.5)	0.49 ± 0.12
		80	H_2O	48.0 ± 1.7	1260 ± 45 (160)	
			CO[e]	14.9 ± 3.5	6.6 ± 1.6 (1.8)	0.53 ± 0.13
		100	H_2O	48.0 ± 1.7	1430 ± 51 (181)	
			CO[e]	14.8 ± 3.5	7.7 ± 1.8 (2.1)	0.54 ± 0.13
		120	H_2O	48.0 ± 1.7	1620 ± 58 (206)	
			CO[e]	14.7 ± 3.5	8.7 ± 2.1 (2.3)	0.53 ± 0.13

[a] Midobserving decimal UT date, heliocentric distance (AU), geocentric distance (AU), and geocentric Doppler shift (km s^{-1}).

[b] Line flux contained within a 1″ × 3″ nucleus-centered aperture. Observations of standard star BS0003 yielded calibration factors [Γ, 10^{-17} W m^{-2} (cm^{-1})$^{-1}$/ (ADU s^{-1})] of 1.818 ± 0.065 and 1.883 ± 0.046 on May 27 and 30, respectively. Uncertainties represent the 1 σ stochastic error (combined CO *R*1+*R*2 entries reflect the larger of stochastic and standard errors).

[c] Global production rate, using q_{scale} = 2.607 ± 0.288 and 1.948 ± 0.351 on May 27 and 30, respectively (see text). The first uncertainty listed is σQ_{stoch} (the larger of σQ_{stoch}, σQ_{std} is listed for CO *R*1+*R*2); the values in parentheses include uncertainties in Γ and q_{scale}.

[d] The relative abundance (i.e., mixing ratio) for CO is independent of uncertainties in Γ and q_{scale}, incorporating only σQ_{stoch} for H_2O and the larger of σQ_{stoch} and σQ_{std} for CO.

[e] Entries for CO include subtraction of modeled intensity from the ν_1–ν_2, 5_{05}–4_{14} line of H_2O at the *R*2 line position. For a given Doppler shift, the contribution from this H_2O line becomes more pronounced with increasing T_{rot}, decreasing CO/H_2O, and decreasing spectral resolving power. For our observations of SW3-C, even the maximum contribution is meager (only ~4% at 120 K on 27 May) because of poor atmospheric transmittance of this line due to accidental overlap with telluric CO (*R*2 line) absorption.

[f] Dependence on rotational temperature.

perature (i.e., H-atom retention time), and on whether the CO is housed structurally with H_2O in the ice (e.g., see Watanabe et al. 2004). One measure of this conversion can be represented by the sum of H_2CO and CH_3OH abundances divided by the sum of all three abundances (DiSanti et al. 2002). This assumes that H_2CO and CH_3OH are the only products and that they derive solely from CO.

This interpretation of the measured abundances may be compromised if icy grains in the inner protosolar nebula were thermally processed prior to their final incorporation into the nucleus. It is possible that the grains in SW3 originally had a higher endowment of CO that later was preferentially lost through vaporization in the subsequent warmer nebular environs. If so, the observed and primordial (precometary) abundances of these three molecules in cometary comae may differ, and the measured conversion efficiency may not accurately reflect natal conditions.

3.2. *Comparison with Other Comets*

The abundances of CO among comets show the largest variation of any parent volatile, spanning more than a factor of 30. However, they are not correlated with CH_4 (also highly volatile) among comets, demonstrating that thermal considerations alone cannot explain molecular abundances in comets (Gibb et al. 2003).

The depleted volatile abundances observed in SW3 are perhaps most similar to those in the long-period (Oort Cloud) comet D/1999 S4 (LINEAR), which also disrupted. Gas-phase processing of ices in the inner giant planets' region (R_h ~ 5–10 AU) was proposed for D/1999 S4 (Mumma et al. 2001) based on its highly depleted CH_3OH but more nearly "normal" HCN (Mumma et al. 2001; Bockelée-Morvan et al. 2001) and H_2S (Bockelée-Morvan et al. 2001). With a mixing ratio of 0.9% ± 0.3% (Mumma et al. 2001), CO was severely depleted in D/1999 S4. This demonstrates that comets belonging to different present-day dynamical reservoirs (Oort Cloud and Kuiper Belt) can display a very similar organic volatile chemistry.

It is also interesting to compare the composition of SW3 with that of the JFC 9P/Tempel 1 (hereafter 9P/T1), target of the *Deep Impact* mission that allowed (presumably less processed) subsurface material to be sampled as a result of a deliberate collision (A'Hearn et al. 2005). Material ejected by the collision differed in chemical composition (volatile abundances) and structure (crystallinity of silicate dust) from that released by ambient activity (Mumma et al. 2005; Harker et al. 2005; Lisse et al. 2006; DiSanti et al. 2007). From NIR spectroscopy (with NIRSPEC at Keck; Mumma et al. 2005), its (modest) CH_3OH abundance (~1%) was unchanged by the impact. CO was measured with NIRSPEC only postimpact, on both July 4 and 5. Its abundance was similar (~4%) on these dates (at the 2–3 σ confidence level; Mumma et al. 2005), and an abundance as high as 10% was reported from *HST* observations prior to and following impact (Feldman et al. 2006). We take these values to represent the mean nuclear mixing ratio, notwithstanding the evidence of chemical heterogeneity among individual vents returned by *Deep Impact* spacecraft measurements (Feaga et al. 2007).

Assuming that no unseen CO-hydrogenation products are present in either comet, these results may indicate different conversion efficiencies for ices in 9P/T1 (~30%) versus SW3-

C (~65%; however, this is based only on upper limits of ~0.5% for the mixing ratios of H_2CO and CH_3OH; Villanueva et al. 2006a).[9] The lower abundances of parent volatiles (relative to H_2O) and the (potentially) greater processing of precometary ices in SW3 may indicate its formation closer to the Sun. Alternatively, it was suggested that SW3 and 9P/T1 may both have formed farther than 5–10 AU from the Sun but that SW3 formed later in time, after significant nebular clearing had allowed penetration of ionizing flux (producing a higher H-atom density) to greater distances with commensurate enhanced processing of its precometary ices (Villanueva et al. 2006a). The abundances of CO in SW3 and 9P/T1 suggest differences in the processing of their ices; however, in the absence of a complete inventory of possible hydrogenation products in these two comets, no firm conclusion can be drawn.

4. SUMMARY

We conducted a sensitive search for CO emission in fragment C of the recently split JFC SW3, using CSHELL at the NASA IRTF to target the *R*1 and *R*2 lines at wavelengths near 4.646 μm. Based on simultaneous detection of H_2O, this revealed a depleted abundance ($CO/H_2O = 0.5\% \pm 0.13\%$), in line with the low abundances measured for most other organic volatiles in SW3. This may indicate gas-phase processing of its precometary ices in the inner giant planets' region of the protosolar nebula, as proposed for the Oort Cloud comet D/1999 S4 (LINEAR), which exhibited similarly depleted volatiles. Depleted CO could also result if SW3 formed farther from the Sun but relatively late, after nebular clearing had allowed significant penetration of high-energy radiation. Regardless, this demonstrates that comets belonging to different present-day dynamical reservoirs can display very similar volatile organic chemistries.

We acknowledge support from the NASA Planetary Astronomy Program under RTOPs 344-32-30-07 and 344-32-98, from the NASA Astrobiology Program under RTOP 344-53-51, and from the National Science Foundation RUI Program (0407052). G. L. V. acknowledges support under the NPP Resident Research Associateship Program managed by ORAU. We thank the IRTF staff for their support, especially Lars Bergknut and Imai Namahoe for a hardware fix to CSHELL that made this investigation possible. The NASA-IRTF is operated by the University of Hawaii under Cooperative Agreement NCC 5-538 with the NASA-OSS Planetary Astronomy Program.

[9] A paper reporting mixing ratios of ~0.1%–0.2% for H_2CO and CH_3OH in SW3 has been accepted for publication (Dello Russo et al. 2007).

REFERENCES

A'Hearn, M. A., et al. 2005, Science, 310, 258
Bernstein, G., Trilling, D. E., Allen, R. L., Brown, M. E., Holam, M., & Malhotra, R. 2004, AJ, 128, 1364
Biver, N., et al. 2002, Earth Moon Planets, 90, 323
———. 2006, BAAS, 38, 484
Blake, G. A., Salyk, C., Bonev, B. P., Villanueva, G. L., DiSanti, M. A., Mumma, M. J., Magee-Sauer, K., & Gibb, E. L. 2006, IAU Circ. 8704
Bockelée-Morvan, D., et al. 2001, Science, 292, 1339
Boehnhardt, H., Holdstock, S., Hainaut, O., Tozzi, G. P., Benetti, S., & Licandro, J. 2002, Earth Moon Planets, 90, 131
Boehnhardt, H., & Kaufl, H. U. 1995, IAU Circ. 6274
Bonev, B. P., Mumma, M. J., DiSanti, M. A., Dello Russo, N., Magee-Sauer, K., Ellis, R. S., & Stark, D. P. 2006, ApJ, 653, 774
Crovisier, J., Bockelée-Morvan, D., Gerard, E., Rauer, H., Biver, N., Colom, P., & Jorda, L. 1996, A&A 310, L17
Crovisier, J., et al. 2006, BAAS, 38, 485
Dello Russo, N., DiSanti, M. A., Magee-Sauer, K., Gibb, E. L., Mumma, M. J., Barber, R. J., & Tennyson, J. 2004, Icarus, 168, 186
Dello Russo, N., Vervack, R. J., Weaver, H. A., Biver, N., Bockelée-Morvan, D., Crovisier, J., & Lisse, C. M. 2006, BAAS, 38, 485
———. 2007, Nature, in press
DiSanti, M. A., Bonev, B. P., Magee-Sauer, K., Dello Russo, N., Mumma, M. J., Reuter, D. C., & Villanueva, G. L. 2006, ApJ, 650, 470
DiSanti, M. A., Dello Russo, N., Magee-Sauer, K., Gibb, E. L., Reuter, D. C., & Mumma, M. J. 2002, in Proc. Asteroids, Comets, Meteors, ACM 2002, ed. B. Warmbein (ESA SP-500; Noordwijk: ESA), 571
DiSanti, M. A., Mumma, M. J., Dello Russo, N., & Magee-Sauer, K. 2001, Icarus, 153, 361
DiSanti, M. A., Villanueva, G. L., Bonev, B. P., Magee-Sauer, K., Lyke, J. E., & Mumma, M. J. 2007, Icarus, 187, 240
Edwards, D. P. 1992, NCAR Tech. Note NCAR/TN-367 STR
Feaga, L. M., A'Hearn, M. F., Sunshine, J. M., Groussin, O., & Farnham, T. L. 2007, Icarus, in press
Feldman, P. D., Lupu, R. E., McCandliss, S. R., Weaver, H. A., A'Hearn, M. F., Belton, M. J. S., & Meech, K. J. 2006, ApJ, 647, L61
Gibb, E. L., Mumma, M. J., Dello Russo, N., DiSanti, M. A., & Magee-Sauer, K. 2003, Icarus, 165, 391
Gibb, E. L., Whittet, D. C. B., Boogert, A. C. A., & Tielens, A. G. G. M. 2004, ApJS, 151, 35
Gladman, B. 2005, Science, 307, 71
Gomes, R., Levison, H. F., Tsiganis, K., & Morbidelli, A. 2005, Nature, 435, 466
Harker, D. E., Woodward, C. E., & Wooden, D. H. 2005, Science, 310, 278
Kawakita, H., Kobayashi, H., & Mumma, M. J. 2006a, BAAS, 38(3), 503
Kawakita, H., et al. 2006b, Cent. Bur. Electron. Tel., 532
Lisse, C. M., et al. 2006, Science, 313, 635
Magee-Sauer, K., Mumma, M. J., DiSanti, M. A., Dello Russo, N., Gibb, E. L., Bonev, B. P., & Villanueva, G. L. 2007, Icarus, submitted
Mumma, M. J., DiSanti, M. A., Dello Russo, N., Magee-Sauer, K., Fomenkova, M., Kaminski, C. M., & Xie, D. X. 1996, Science, 272, 1310
Mumma, M. J., DiSanti, M. A., Dello Russo, N., Magee-Sauer, K., Gibb, E. L., & Novak, R. 2003, Adv. Space Res., 31, 2563
Mumma, M. J., Villanueva, G. L., Bonev, B. P., DiSanti, M. A., Magee-Sauer, K., Salyk, C., & Blake, G. A. 2006, BAAS, 38(3), 486
Mumma, M. J., et al. 2001, Science, 292, 1334
———. 2005, Science, 310, 270
Rothman, L. S., et al. 2005, J. Quant. Spectrosc. Radiat. Transfer, 96, 139
Salyk, C., Blake, G. A., Boogert, A. C., & Brown, J. M. 2006, BAAS, 38(3), 506
Shuping, R. Y., Chiar, J. E., Snow, T. P., & Kerr, T. 2001, ApJ, 547, L161
Tokunaga, A. T., Toomey, D. W., Carr, J., Hall, D. N., & Epps, H. W. 1990, Proc. SPIE, 1235, 131
Villanueva, G. L., Bonev, B. P., Mumma, M. J., Magee-Sauer, K., DiSanti, M. A., Salyk, C., & Blake, G. A. 2006a, ApJ, 650, L87
Villanueva, G. L., et al. 2006b, BAAS, 38(3), 485
Watanabe, N., Nagaoka, A., Shiraki, T., & Kouchi, A. 2004, ApJ, 616, 638
Weaver, H. A., Feldman, P. D., Combi, M. R., Krasnopolsky, V., Lisse, C. M., & Shemansky, D. E. 2002, ApJ, 576, L95
Weaver, H. A., Lisse, C. M., Mutchler, M. J., Lamy, P., Toth, I., & Reach, W. T. 2006, BAAS, 38(3), 490
Weaver, H. A., et al. 2001, Science, 292, 1329